V European Conference on Computational Fluid Dynamics
ECCOMAS CFD 2010
J. C. F. Pereira and A. Sequeira (Eds)
Lisbon, Portugal,14-17 June 2010

TWO NUMERICAL SCHEMES FOR SIMULATION OF THE STRATIFIED FLOWS PAST A MOVING BODY

L. Beneš[*], J. Fürst[†], Ph. Fraunié[‡]

[*],[†] Dept. of Technical Mathematics,
Fac. of Mechanical Engineering, CTU Prague
Karlovo nám. 13, Prague 2, 121 35
e-mail: benes@marian.fsik.cvut.cz
e-mail: furst@marian.fsik.cvut.cz
[‡]LSEET/CNRS
Université de Toulon et du Var, France
e-mail: Philippe.Fraunie@lseet.univ-tln.fr

Key words: Stratified flow, Boussinesq approximation, AUSM MUSCL, WENO, Artificial compressibility, Internal waves

Abstract. *The article deals with the numerical simulation of the flow pattern around a moving body in a stratified fluid. The flow is assumed to be unsteady, incompressible and stratified. Initial system of equations is the Boussinesq approximation of the Navier–Stokes equations. The flow field in the towing tank with a moving sphere and flat strip is modeled for a wide range of Richardson numbers. The obstacle is modeled via penalization technique. The resulting set of partial differential equations is then solved by the fifth-order finite difference WENO scheme, or by the second-order finite volume AUSM MUSCL scheme. For the time integration, the second-order BDF method was used. Both schemes are combined with the artificial compressibility method in dual time.*

1 Introduction

Stratification plays important role in many industrial and environmental problems. Thoroughly study of the effect of stratification leads to a better modeling and finally to a better understanding of these processes. Since this is a very complicated problem, study of the simplified cases has a long tradition. One of the most popular cases is the moving body in stratified medium. The flow structure around a uniformly moving obstacle is subject of intensive numerical and experimental studies. This investigation help us to better understanding nature of the stratified flow and re-structuring with changing of the flow parameters. The processes occurring from the impulsive started body up to formation of internal waves are computed.

2 Boussinesq approximation

For description of this type of flow, the Navier-Stokes equations for viscous incompressible flow with variable density in 2D are used. These equations are simplified by the Boussineq approximation. Density and pressure are divided into two parts: a background field (with subscript $_0$) plus a perturbation. The background field fulfill the hydrostatic balance equation $\partial p_0(z)/\partial y = -\rho_0(y)g$. The system of equations obtained is partly linearized around the average state ρ_*. The resulting set of equations can be written in the form

$$PW_t + F^i(W)_x + G^i(W)_y = \nu(F^v(W)_x + G^v(W)_y) + S(W). \tag{1}$$
$$F^i = [\rho u, u^2 + \frac{p}{\varrho_*}, uv, u]^T,\ G^i = [\rho v, uv, v^2 + \frac{p}{\varrho_*}, v]^T,$$
$$F^v = [0, u_x, v_x, 0]^T, \quad G^v = [0, u_y, v_y, 0]^T.$$

where $W = [\rho, u, v, p]^T$, is vector of unknown variables respectively, the density perturbation, three velocity components and the pressure perturbation. $S = [-vd\rho_0/dy, 0, -g, 0]^T$ is the gravity and source term and $P = diag(1, 1, 1, 0)$. To describe the stratification, the following parameters were used. An exponential profile $\varrho_0 = \varrho_{00}\exp(y/\Lambda)$ of the undisturbed density is characterized by a constant length scale of stratification $\Lambda = 1/\frac{d\ln\varrho}{dy}$ where $\varrho_{00} = \varrho_0(0)$ is a reference density, buoyancy frequency $N = 2\pi/T_b = \sqrt{g/\Lambda}$ where T_b is a buoyancy frequency and bulk Richardson number

$$Ri = \frac{g\frac{d\rho_0}{dy}}{\varrho_* U^{ob^2}}$$

whereU^{ob} is velocity of the moving obstacle.

3 Numerical schemes

Two different numerical schemes were used. The time discretization is the same in both cases. For the spatial were used either the flux-splitting method with WENO interpolation or the finite volume AUSM MUSCL scheme with the Hemker-Koren limiter.

3.1 Flux splitting for incompressible flows

The discretization in space is achieved by standard fourth-order differences for viscous terms. For discretization of the inviscid fluxes the high-order flux-splitting method of the following form was used. Divide the inviscid flux $F^{in}(W)$ into two parts, the convective flux $F^c(W) = [\rho u, u^2, uv, 0]^T$ and the pressure flux $F^p(W) = [0, p, 0, \beta^2 u]^T$, then approximate the flux derivative by

$$F^i(W)_x\big|_i \approx \frac{1}{\Delta x}\left[F^c_{i+1/2} - F^c_{i-1/2}\right] + \frac{1}{\Delta x}\left[F^p_{i+1/2} - F^p_{i-1/2}\right]. \tag{2}$$

The high-order weighted ENO scheme[11] is chosen as the interpolation method (only the spatial index i in the x– direction is preserved). The original WENO interpolation uses an upwind bias and it can be formally written in the following form (function `weno5` is described in[11]):

$$\phi_{i+1/2} = \begin{cases} \phi^+_{i+1/2} = \texttt{weno5}(\phi_{i-2}, \phi_{i-1}, \phi_i, \phi_{i+1}, \phi_{i+2}) & \text{if } u_{i+1/2} > 0, \\ \phi^-_{i+1/2} = \texttt{weno5}(\phi_{i+3}, \phi_{i+2}, \phi_{i+1}, \phi_i, \phi_{i-1}) & \text{if } u_{i+1/2} \le 0. \end{cases} \tag{3}$$

The final scheme can be written in the form

$$u_{i+1/2} := (u^+_{i+1/2} + u^-_{i+1/2})/2, \quad p_{i+1/2} := (p^+_{i+1/2} + p^-_{i+1/2})/2, \tag{4}$$

$$F^c(W)_{i+1/2} := ((\rho u)^\pm_{i+1/2}, (u^2)^\pm_{i+1/2}, (uv)^\pm_{i+1/2}, (uw)^\pm_{i+1/2}, 0)^T$$

$$F^p(W) := (0, p_{i+1/2} + \beta\frac{u^+_{i+1/2} - u^-_{i+1/2}}{2}, 0, 0, u_{i+1/2} + \frac{p^+_{i+1/2} - p^-_{i+1/2}}{2\beta})^T,$$

where $+$ or $-$ is taken in the convective flux according to the sign of $u_{i+1/2}$.

A similar algorithm is applied for the fluxes G. The resulting scheme has high-order accuracy in space. It was validated for the case of compressible inviscid flows by a computation of shock-vortex interaction; see[10].

3.2 AUSM scheme

The finite volume AUSM scheme was used for spatial discretization of the inviscid fluxes in our second scheme.

$$\begin{aligned} \int_\Omega (F^i_x + G^i_y)dS &= \oint_{\partial\Omega} (F^i n_x + G^i n_y)dl \\ &\approx \sum_{k=1}^{4} \left[u_n \begin{pmatrix} \varrho \\ u \\ v \\ \beta^2 \end{pmatrix}_{L/R} + p \begin{pmatrix} 0 \\ n_x \\ n_y \\ 0 \end{pmatrix} \right] \Delta l_k, \end{aligned} \tag{5}$$

where n is the normal vector, u_n the normal velocity vector, and $(q)_{L/R}$ are quantities on the left/right hand side of the face. These quantities are computed using MUSCL reconstruction with the Hemker-Koren limiter[9] in the form[4]:

$$q_R = q_{i+1} - \frac{1}{2}\delta_R, \quad q_L = q_i + \frac{1}{2}\delta_L,$$

$$\delta_{L/R} = \frac{a_{L/R}(b_{L/R}^2 + 2) + b_{L/R}(2a_{L/R}^2 + 1)}{2a_{L/R}^2 + 2b_{L/R}^2 - a_{L/R}b_{L/R} + 3},$$

$$a_R = q_{i+2} - q_{i+1}, \quad a_L = q_{i+1} - q_i, \quad b_R = q_{i+1} - q_i, \quad b_L = q_i - q_{i-1}.$$

Since the pressure is discretized using central differences, the scheme is stabilized following[5] by a pressure diffusion of the form

$$F_{\mathbf{d}i+1/2,j} = \left(0,\ 0,\ 0,\ \eta\frac{p_{i+1,j} - p_{i,j}}{\beta_x}\right)^T, \qquad \beta_x = w_r + \frac{2\nu}{\Delta x}$$

where T denotes transpose and w_r is a reference velocity (in our case the maximum velocity in the flow field). Viscous fluxes are discretized using central differences on the dual mesh. This scheme is second-order accurate in space.

3.3 Time integration

The spatial discretization yields a system of ODE in the physical time t variable, which is solved by the second-order BDF formula

$$P\frac{3W^{n+1} - 4W^n + W^{n-1}}{2\Delta t} + (\tilde{F}_x^i + \tilde{G}_y^i +)(W^{n+1}) - \nu(\tilde{F}_x^v + \tilde{G}_y^v +)(W^{n+1}) = \tilde{S}^{n+1}. \qquad (6)$$

By $\tilde{}$ is denoted above described numerical approximation of the fluxes. Arising set of equations is solved by an artificial compressibility method in the dual time τ by an explicit 3-stage second-order Runge-Kutta method of the second order.

4 Obstacle modeling

Our computations are focused to the modeling of the flows past a moving body. There are various possibilities how to model body (e.g. moving mesh, immersed boundary see[8]). In our computations, the obstacle is modeled using by penalization technique as a source term emulating a porous media with high resistance. The source term $S(W)$ in this case takes the form

$$\left[-w\frac{d\rho_0}{dz}, 0, -g, 0\right]^T + \frac{\chi(x,y,z,t)}{K}\left[0, U^{ob} - u, V^{ob} - v, 0\right]^T, \qquad (7)$$

where K corresponds to small permeability and $\chi(x,y,t)$ is the characteristic function of the obstacle, which moves with velocity (U^{ob}, V^{ob}).

To estimate the influence of the permeability K, and also numerical tests were published in[1].

5 Numerical results

Laboratory studies of flow around the body and produced internal waves has a long tradition. It was recognized in experiments and theory that the flow pattern around obstacles in a deep continuously stratified fluid depends on internal Froude number

$$Fr = \frac{U^2}{N^2 D^2}$$

where U is the flow velocity and D vertical size of obstacle. When the Froude number is large, relatively long internal waves are generated which are located mostly past the obstacle. On the other hand, when the Froude number is small, the upstream disturbance is pronounced.

5.1 Flow past a moving sphere

The first validation of the schemes mentioned above was performed by the simulation of the towing tank problem with moving sphere. The towing tank is a brimfull channel with the moving obstacle inside. Other physical parameters are: dimensions $8 \times 4m$ in 2D or $8 \times 4 \times 1m$ in 3D, $\rho_* = 1\ kg/m^3$, the kinematic viscosity $\nu = 10^{-4}\ m^2/s$ and stable density gradient $d\rho_0/dy = -0.1\ kg/m^4$. The obstacle is a sphere of radius $0.1\ m$, located $1m$ from the left wall and at the middle of height and width. At time $t = 0$ the obstacle starts moving with constant velocity $U^{ob} = 1\ m/s$ in the x direction.

Homogeneous Dirichlet boundary conditions for the velocity and Neumann conditions for the density and pressure disturbances were used. Cartesian grid with 320×160 cells was used. The simulations were performed for wide range of stratifications $Ri \in < 0, 100 >$.

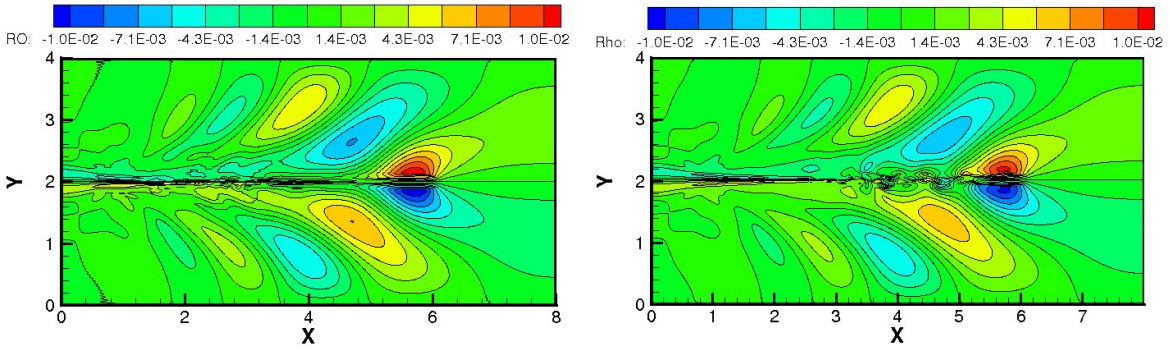

Figure 1: Comparison of isolines of the density disturbances at the time $t = 5s$, $g = 100$, $Ri = 10$. AUSM MUSCL scheme left and WENO5 right.

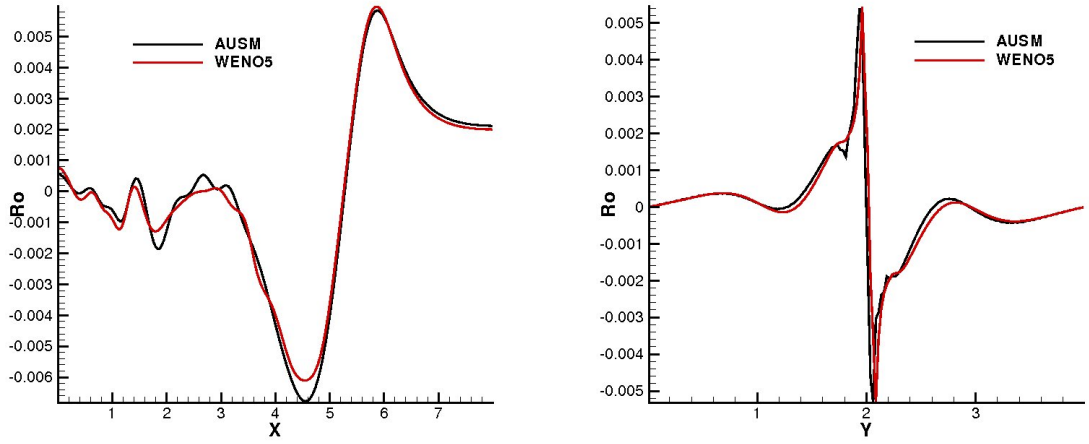

Figure 2: Comparison of both schemes. Longitudinal (left) and transversal (right) distribution of the ρ (right) $Ri = 10$, time $t = 5s$.

In the figures 1,2 we can see comparison of the schemes in 2D in the form of density isolines and longitudinal and transversal distribution of the density perturbance. Performed computations exhibit good agreement between both methods. For more information, testing of the influence of mesh and permeability parameter see our previous studies,[7],[1].

5.2 Flow around moving strip

As a second case, the flow around the moving vertical strip was studied. A vertical strip of the height $h = 2.5cm$ and thickness $0.43cm$ is placed vertically in the tank of dimension $2.2 \times 0.6m$. Starting position $1m$ from the left and in the center of the height. Coordinate system is placed to the center of the obstacle in the starting time. At time $t = 0$ the obstacle starts moving with constant velocity $U^{ob} = 0.0026\ m/s$. Other parameters: $\rho_{00} = 1008.9kg/m^3$, the kinematic viscosity $\nu = 10^{-6}\ m^2/s$ and length scale of stratification $\Lambda = 38.75$. Cartesian grids with 514×602 cells and 1500×602 cells were used.

First of all, when impulsively started, the vertical body generates an initial perturbation which is presented in the sequence of fig. 3. The temporal evolution of the v-velocity component for three times $t = 16.5, 49.4, 82.3s$, which corresponds to the nondimensional time $t/T_b = 1.32, 3.96, 6.6$ describe process of wave generation.

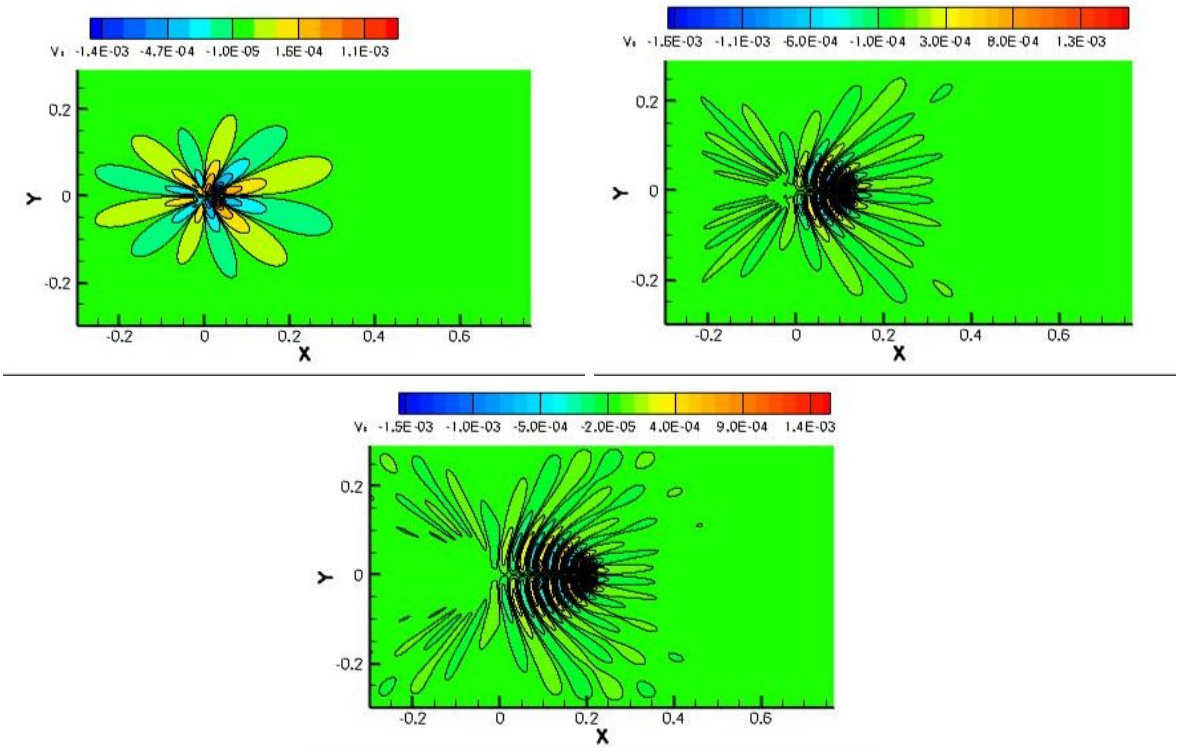

Figure 3: Evolution of the v-velocity component for three different times $t = 16.5, 49.4, 82.3s$. Zoom view close to the strip.

Next fig. 4 shows distribution of density (left) and density gradient $\frac{\partial \varrho}{\partial x}$. The displacement of isolines visualizes the location of the Lee wave crests and troughs. Wave field is antisymmetric with respect to the $x-$axis.

Figure 5 shows flow structure in the form of Schlieren image obtained by Chashechkin and Mitkin[6]. In this type of flow image, the illumination is proportional to the horizontal component of index of refraction and is linearly connected with density gradient. Black and white strips displays crests and troughs of internal waves. The flow structure corresponds to computed flow field in fig.4.

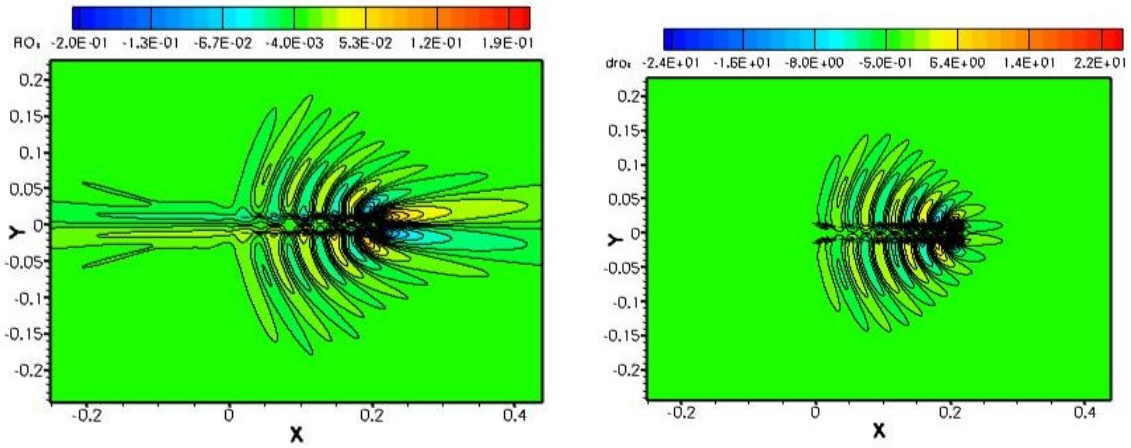

Figure 4: Density disturbance (left) and density gradient $\frac{\partial \varrho}{\partial x}$ (right) at given time $t = 82.3s$. Zoom view close to the strip.

On the last figure 5, the comparison with computation performed by Houcine and Fraunié is presented[3]. Figures shows isolines of gradient of u-velocity component $\frac{\partial u}{\partial x}$ at a time $t = 82.3s$. The wave structure with the frequency given by the buoyancy frequency is clearly visible. Another domain with significant gradient occupies strip around the x–axis. Frequency of oscillations is given by the buoyancy frequency too.

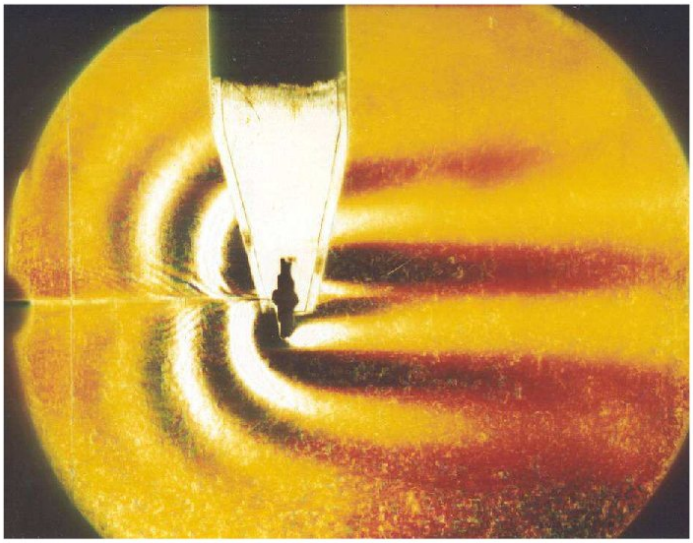

Figure 5: Schlieren image of stratified flow past vertical strip.

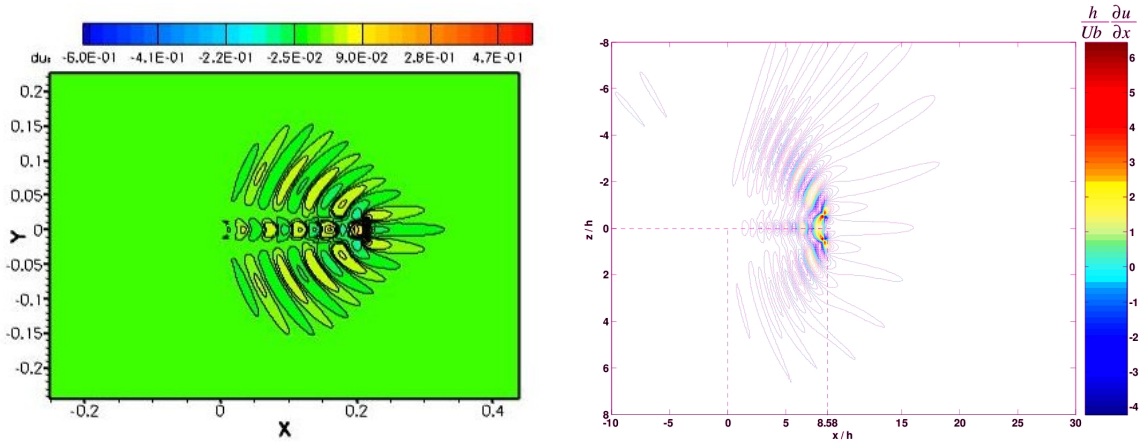

Figure 6: Gradient of u-velocity component $\frac{\partial u}{\partial x}$ at a given time $t = 82.3s$. Our computation (left) and computation of Houcine

6 Conclusion

The flow patterns produced by a moving sphere and vertical strip in stratified medium were computed and compared.

Two numerical methods for simulation of 2D and 3D stratified flows have been developed and compared. Since the solution can depend on the numerical scheme, mesh etc, a comparison of solutions obtained using different methods eliminates this dependence. These results are in good mutual agreement. Quantitative and qualitative agreement both methods and also with experiment and independent computation were demostrated. Small differences that emerged between schemes require deeper investigation.

Acknowledgments: This work was supported by Research Plans MSM 6840770003, MSM 6840770010 and GACR 201/08/0012.

References

[1] Beneš L., Fürst J., Fraunié Ph.: Numerical simulation of the towing tank problem using high order schemes. BAIL 2008 - Boundary and Interior Layers. *Lecture Notes in Computational Science and Engineering 69*, Springer 2009 ISSN 1439-7358.

[2] Berrabaa S., Fraunié P., Crochet M.: 2D Large Eddy Simulation of highly stratified flows : the stepwise structure effect. *Advances in Computation . Scientific Computing and Applications*, volume **7**, 179–185 (2001) Nova Science Publishers

[3] Houcine H., Chaschechkin Yu. D., Fraunié Ph., Fernando H.J.S., Gharbi A., Lili T.: Numerical modelling of the generation of internal waves by uniform stratified flow over a thin vertical barrier. Submitted

[4] Blazek J.: Computational Fluid Dynamics: Principles and Applications. *Elsevier Science 2001*, ISBN 0080430090.

[5] Dick E., Vierendeels J., Riemslagh K.: A multigrid semi–implicit line–method for viscous incompressible and low–mach–number flows on high aspects ratio grids. *Journal of Computational Physics* **154** 310–341 (1999)

[6] Chaschechkin Y.D., Mitkin V.V.: Experimental study of a fine structure of 2D wakes and mixing past an obstacle in a continuously stratified fluid. *Dyn. Atmos. Oceans* 34, 165–187, 2001

[7] Fraunie Ph., Beneš L., Fürst J.: Numerical simulation of the stratified flow. In: Proceeding of conference Topical Problems of Fluid Mechanics 2008, 5–8 (2008)

[8] Fuka V., Brechler J.: LES of contaminant dispersion in an idealized geometry. Proceeding of *CMFF09*, 138–142, Budapest 2009, Hungary ISBN 978-963-420-984-3

[9] Hemker P.W., Koren B.: Multigrid, defect correction and upwind schemes for the steady Navier-Stokes equations. Numerical methods for fluid dynamics III; *Clarendon Press/Oxford University Press*, 1988, p. 153-170.

[10] Kozel K., Angot Ph., Fürst J.: TVD and ENO schemes for multidimensional steady and unsteady flows. In: *Finite Volumes for Complex Applications*, 283–290 Hermes, (1996)

[11] Shu Chi-Wang, Jiang Guang-Shan: Efficient implementation of weighted eno schemes. *Journal of Computational Physics*, **126** 202–228 (1996)